An Interoperable Electric Vehicle Wireless Charging System Based on Mutually Spliced Double-D Coil

Wenbin Pan, Chao Liu, Hongmin Tang, Yizhan Zhuang, *Member, IEEE*, and Yiming Zhang, *Senior Member, IEEE*

***Abstract*—Interoperability and misalignment tolerance issues are two urgent problems to be solved in electric vehicles wireless charging systems. To address these issues, a wireless power transfer (WPT) system based on decoupled mutually spliced double-D (DD) receiving coils is proposed in this article, which can achieve certain interoperability and antimisalignment performance. These two receiving coils are connected in series via the rectifiers on the dc side, resulting in the total equivalent mutual inductance equal to the sum of the absolute values of the mutual inductances between the transmitting coil and the two receiving coils. Compared with existing works, the proposed WPT system can achieve interoperability and misalignment tolerance with different transmitting coils: the square coil, the DD coil along the *X*- or *Y*-directions, and the quadrupole coil. A mathematical model and an experimental prototype are developed to verify the effectiveness of the proposed scheme, and the highest efficiency of the experimental prototype is 92.49%.**

***Index Terms*—Antimisalignment, decoupled, double spliced double-D (DD) coil, interoperability, wireless charging, wireless power transfer (WPT).**

I. Introduction

With the rapid development of electric vehicles (EVs), the charging problem of EVs also needs to be further studied. At present, there are two mainstream charging methods for EVs, which are wired charging and wireless charging. Wired charging is a more traditional solution, the advantages of which are mainly higher efficiency and simpler technology, but the disadvantages are also very obvious: the charging process requires manual intervention, which is not intelligent and automatic enough; it is easy to occur in extreme weather such as heavy rain and snowstorm; at the same time, the length of the wire limits the range of charging and so on. In contrast, wireless charging, also known as wireless power transfer (WPT), has received widespread attention and is favored by academia and industry because of its advantages of reliability, safety, convenience, and automation in transmitting power [1], [2], [3], [4], [5].

Manuscript received 4 October 2023; revised 24 November 2023; accepted 16 December 2023. Date of publication 19 December 2023; date of current version 26 January 2024. This work was supported in part by the National Natural Science Foundation of China under Grant 52107183 and in part by the Natural Science Foundation of Fujian Province under Grant 2022J06011. Recommended for publication by Associate Editor C. Lee. *(Corresponding authors: Yiming Zhang; Yizhan Zhuang.)*

The authors are with the School of Electrical Engineering and Automation, Fuzhou University, Fuzhou 350108, China (e-mail: 210120060@fzu.edu.cn; 220110002@fzu.edu.cn; 220127089@fzu.edu.cn; zyz_joe@fzu.edu.cn; zym@fzu.edu.cn).

Color versions of one or more figures in this article are available at https://doi.org/10.1109/TPEL.2023.3344663.

Digital Object Identifier 10.1109/TPEL.2023.3344663

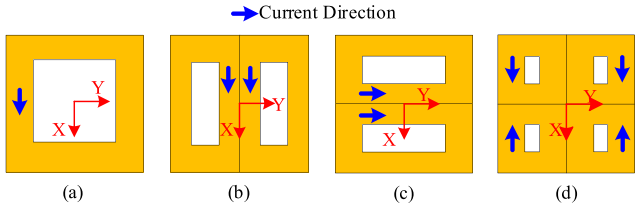

Fig. 1. Conventional coil structures. (a) Square coil. (b) DD coil along *X*-direction. (c) DD coil along *Y*-direction. (d) Quadrupolar coil.

Wireless charging can be classified into many types, among which the most technically mature and widely used is magnetic induction based on coupled coils. The coupled coils are physically separate, resulting in issues such as interoperability [6], [7], [8] and misalignment tolerance [9], [10], which should be solved before successful commercialization. Interoperability refers to the ability to transmit power efficiently between various coil structures, topologies, and other different conditions. Coil interoperability is one key issue. Among them, several coil structures, namely the square coil, the double-D (DD) coils along the *X*- or *Y*-directions, and the quadrupolar coil, are shown in Fig. 1, which are the mainstream structures presently. These coils are decoupled from each other when aligned, leading to failure of efficient power transmission.

Numerous solutions to the interoperability issue have been put up by researchers both domestically and internationally. According to [11] and [12], interoperability could be achieved by maintaining specific relative locations for the transmitting (Tx) and receiving (Rx) coils. However, this approach makes it necessary to charge various coil types at various locations, which is both difficult and unworkable. This is due to the possibility that many EV consumers are unaware of the category to which the charging coil belongs. Therefore, it is crucial to make sure the system can charge various coils simultaneously at the same location. In order to achieve interoperability, [13] published a three-coil interleaved structure, [14] coupled DD coils and solenoid coils, and [15] stacked square coils and DD coils together. The interoperability of a number of the common coil configurations depicted in Fig. 1 cannot be concurrently satisfied by any of these articles, despite the fact that they all manage interoperability to some degree. Further study on coupling structure compatibility is urgently needed since it will have a significant impact on the EV manufacturers and user

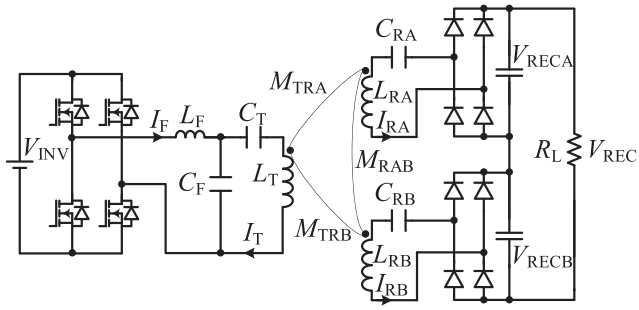

Fig. 2. Proposed system topology.

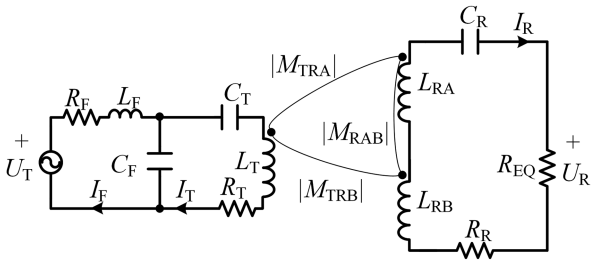

Fig. 3. Equivalent circuit of proposed system.

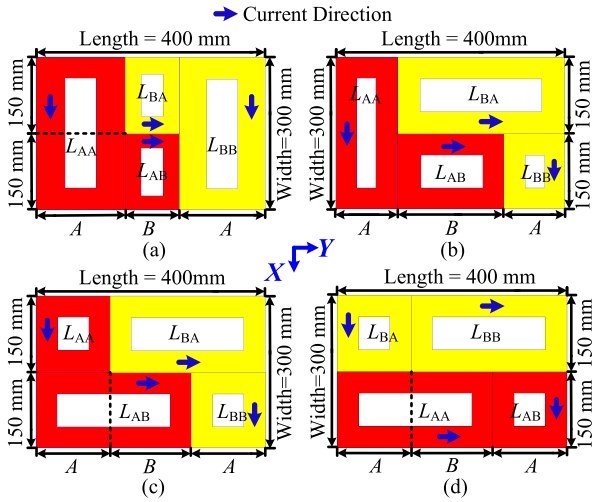

Fig. 4. Proposed coil structures. (a) Structure I. (b) Structure II. (c) Structure III. (d) Structure IV.

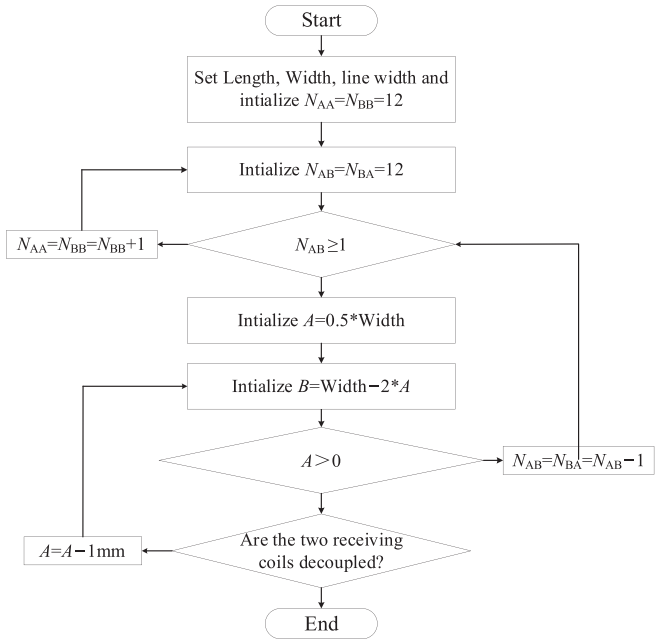

Fig. 5. Proposed coil design flow for decoupling.

groups who employ that coil structure when one of the coil interoperability requirements is not met.

In addition, academics domestically and internationally have conducted a significant amount of research on the performance indices and evaluation methodologies of interoperability in order to ascertain whether the system complies with the interoperability standards [16], [17], [18], [19], [20]. Power and efficiency continue to be the foundation of the most popular and natural evaluation approach. This method generally requires the system to have a certain misalignment tolerance [21], [22], [23]. The reason for the misalignment tolerance is that there is no assurance that the receiver (Rx) side and the transmitter (Tx) side are constantly lined up while a car is parked. During manually operated parking, the Tx and Rx coils may inevitably be out of alignment. Misalignment is a crucial reception problem that must be resolved in order for the system to continue transmitting energy effectively. Because the door–door direction is frequently more prone to misalignment and more challenging to fix than the front-rear direction, misalignment tolerance in the door–door direction is more crucial.

In order to enhance the misalignment tolerance, scholars from various countries have conducted a lot of researches, and various researches mainly focus on three aspects of magnetic coupling structure, compensation topology, and control methods. In terms of magnetic coupler design, multiple coil structures [24] were adopted, such as bipolar coils [25], tripolar coils, DDQ coils, solenoidal coils, and other coil structures [26]. Antiparallel windings [27], [28] can also help to improve the misalignment tolerance. In terms of compensation networks, many studies used hybrid topologies to achieve antimisalignment performance [29], [30], such as series–series and double-sided *LCC* (inductor-capacitor-capacitor) hybrid topologies. On the control system side, it is often implemented by using an additional power conversion stage [31]. With these methods, the misalignment tolerance problem can be solved, but the methods to change the system topology and control system are too complicated. Other studies of optimized coil structures, with fewer coil degrees of freedom, are unable to meet requirements other than resistance to misalignment. Therefore, a simpler and more malleable coil structure is needed to meet the interoperability requirements required in this article with some misalignment tolerance.

To solve these problems, this article proposes a mutually spliced DD coil set, realizing the interoperability of the four prevailing coils, as shown in Fig. 1. Also, the proposed coil structure has certain antimisalignment performance.

The rest of this article is organized as follows. Section II presents the proposed system topology and mathematical model.

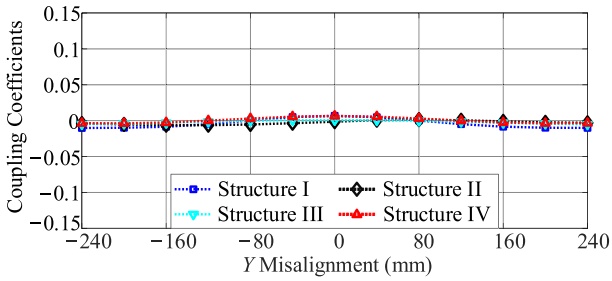

Fig. 6. Variation of the coupling coefficient between Coil A and Coil B with misalignment. (a) Structure I. (b) Structure II. (c) Structure III. (d) Structure IV.

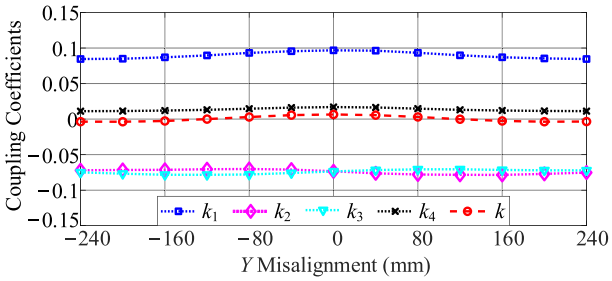

Fig. 7. Coupling coefficients among winding.

The proposed coil structure is presented in Section III, and its interoperability and resistance to misalignment are analyzed. Section IV offers the experimental validation. Finally, Section V concludes this article.

II. Topology and Modelling

The system topology is shown in Fig. 2. V_{INV} (V_{REC}) is the inverter (rectifier) dc voltage. L_{T} is the self-inductance of the Tx coil, and I_{T} is its current. L_{F} is the compensation inductor, and I_{F} is its current. C_{T} is the series compensation capacitor, and C_{F} is the shunt compensation capacitor. C_{RA} and C_{RB} are the Rx series compensation capacitors. L_{RA} and L_{RB} are the self-inductances of the Rx Coils A and B, and I_{RA} and I_{RB} are the Rx coil currents. R_{L} is the load resistance. M_{TRA} (M_{TRB}) is the mutual inductance between the Tx coil and the Rx Coil A (B). M_{RAB} is the mutual inductance between the two Rx coils.

The system works at the resonant angular frequency ω

$$\omega = \frac{1}{\sqrt{L_{\mathrm{RA}}C_{\mathrm{RA}}}} = \frac{1}{\sqrt{L_{\mathrm{RB}}C_{\mathrm{RB}}}} = \frac{1}{\sqrt{L_{\mathrm{T}}\frac{C_{\mathrm{F}}C_{\mathrm{T}}}{C_{\mathrm{F}}+C_{\mathrm{T}}}}}. \tag{1}$$

The equivalent circuit is shown in Fig. 3. R_{F} is the equivalent series resistance (ESR) of L_{F}. R_{T} is the ESR of L_{T}. R_{R} is the sum of the ESRs of L_{RA} and L_{RB}. C_{R} is the series equivalent capacitance of C_{RA} and C_{RB}. R_{R} and C_{R} can be expressed as

$$R_{\mathrm{R}} = R_{\mathrm{RA}} + R_{\mathrm{RB}}, C_{\mathrm{R}} = \frac{C_{\mathrm{RA}}C_{\mathrm{RB}}}{C_{\mathrm{RA}}+C_{\mathrm{RB}}}. \tag{2}$$

U_{T} (U_{R}) is the fundamental component of the inverter (rectifier) ac voltage. R_{EQ} is the equivalent load resistance. U_{T}, U_{R}, and R_{EQ} can be expressed as

$$U_{\mathrm{T}} = \frac{2\sqrt{2}}{\pi}V_{\mathrm{INV}}, U_{\mathrm{R}} = \frac{2\sqrt{2}}{\pi}V_{\mathrm{REC}}, R_{\mathrm{EQ}} = \frac{8}{\pi^2}R_{\mathrm{L}}. \tag{3}$$

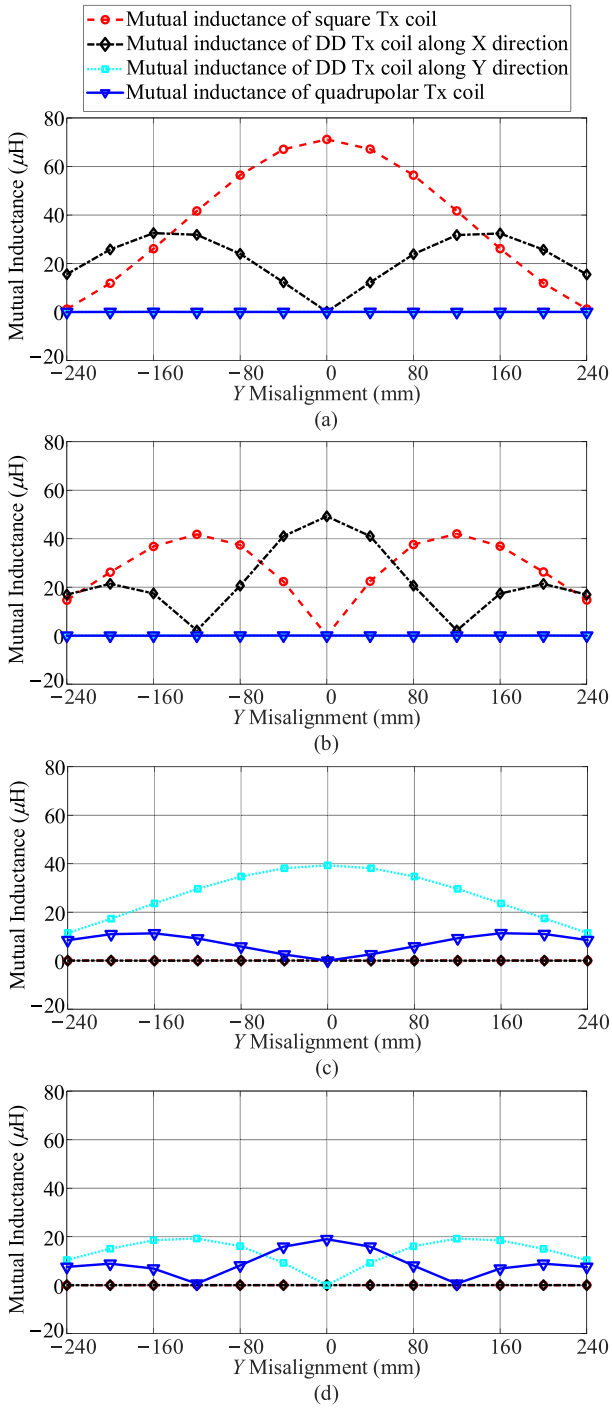

Fig. 8. Variation of mutual inductance with misalignment between different Tx and Rx coils when the Rx coil is a conventional coil structure. (a) Square Rx coil. (b) DD Rx coil along *X*-direction. (c) DD Rx coil along *Y*-direction. (d) Quadrupolar Rx coil.

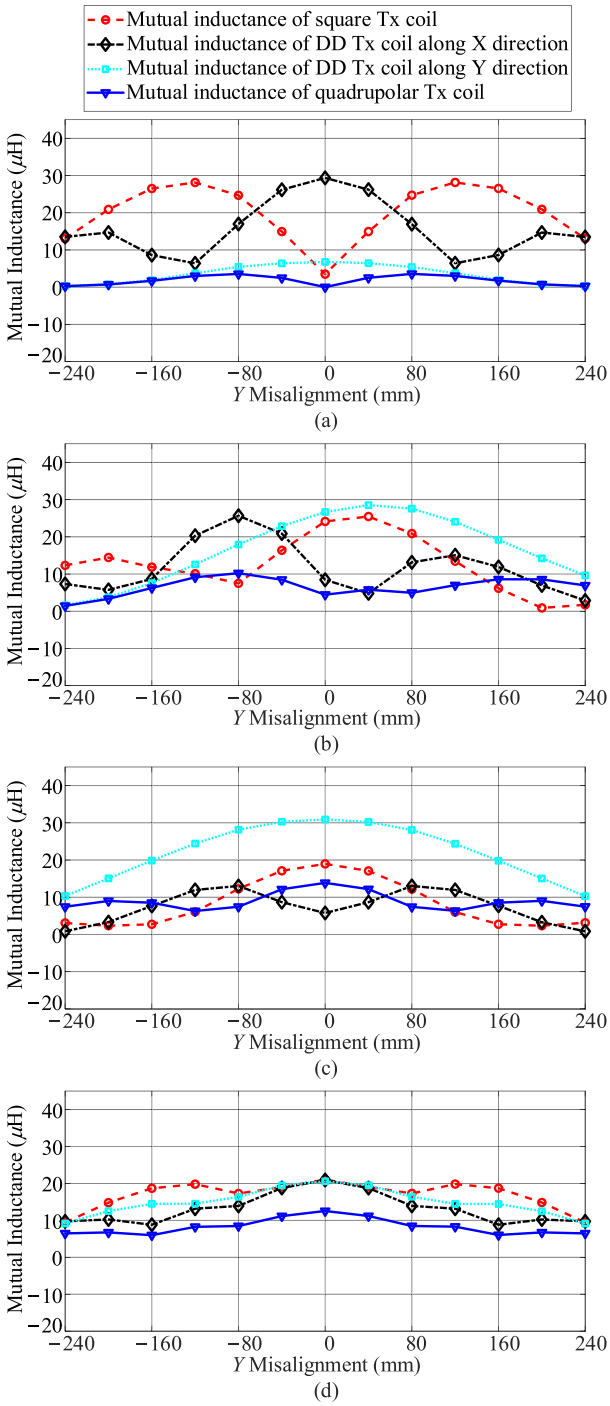

Fig. 9. Variation of mutual inductance with misalignment when the Rx coil is the proposed coil or the conventional coil. (a) Structure I. (b) Structure II. (c) Structure III. (d) Structure IV.

At the resonant frequency, according to Kirchhoff's voltage law, one can get

$$\begin{cases} \dot{U}_{\mathrm{T}} = \left(R_{\mathrm{F}} + j\omega L_{\mathrm{F}} + \frac{1}{j\omega C_{\mathrm{F}}}\right)\dot{I}_{\mathrm{F}} - \frac{1}{j\omega C_{\mathrm{F}}}\dot{I}_{\mathrm{T}} \\ 0 = -\frac{1}{j\omega C_{\mathrm{F}}}\dot{I}_{\mathrm{F}} + \left(R_{\mathrm{T}} + j\omega L_{\mathrm{T}} + \frac{1}{j\omega C_{\mathrm{T}}} + \frac{1}{j\omega C_{\mathrm{F}}}\right)\dot{I}_{\mathrm{T}} \\ \quad -j\omega M_{\mathrm{TR}}\dot{I}_{\mathrm{R}} \\ 0 = (j\omega L_{\mathrm{RA}} + \frac{1}{j\omega C_{\mathrm{R}}} + j\omega L_{\mathrm{RB}} + R_{\mathrm{R}} + R_{\mathrm{EQ}} \\ \quad +2j\omega M_{\mathrm{RAB}})\dot{I}_{\mathrm{R}} - j\omega M_{\mathrm{TR}}\dot{I}_{\mathrm{T}} + \frac{8\sqrt{2}}{\pi}V_{\mathrm{on}} \end{cases} \tag{4}$$

TABLE I
COIL SIZE AND NUMBER OF TURNS

	Structure I	Structure II	Structure III	Structure IV
A	154 mm	103 mm	136 mm	127 mm
B	92 mm	194 mm	128 mm	146 mm
N_{AA}	13	12	12	12
N_{AB}	8	12	12	12
N_{BB}	13	12	12	12
N_{BA}	8	12	12	12

in which M_{TR} is the sum of the absolute values of M_{TRA} and M_{TRB}, namely

$$M_{\mathrm{TR}} = |M_{\mathrm{TRA}}| + |M_{\mathrm{TRB}}|. \tag{5}$$

According to the abovementioned equation, it can be obtained

$$\begin{cases} I_{\mathrm{R}} = \frac{\alpha M_{\mathrm{TR}} U_{\mathrm{T}} - \frac{8\sqrt{2}}{\pi}V_{\mathrm{on}}}{\sqrt{\left[R_{\mathrm{R}} + R_{\mathrm{EQ}} + \alpha(\omega M_{\mathrm{TR}})^2 C_{\mathrm{F}} R_{\mathrm{F}}\right]^2 + (2\omega M_{\mathrm{RAB}})^2}} \\ I_{\mathrm{T}} = \alpha C_{\mathrm{F}} R_{\mathrm{F}}\left(\omega M_{\mathrm{TR}} I_{\mathrm{R}} - \frac{U_{\mathrm{T}}}{\omega C_{\mathrm{F}} R_{\mathrm{F}}}\right), I_{\mathrm{F}} = \frac{U_{\mathrm{T}}}{R_{\mathrm{F}}} + \frac{I_{\mathrm{T}}}{\omega C_{\mathrm{F}} R_{\mathrm{F}}} \end{cases} \tag{6}$$

where α is defined as follows:

$$\alpha = \frac{1}{L_{\mathrm{F}} + R_{\mathrm{T}} R_{\mathrm{F}} C_{\mathrm{F}}}. \tag{7}$$

The output voltage, output power, and the efficiency can be obtained as

$$U_{\mathrm{OUT}} = \frac{\frac{\pi}{2\sqrt{2}}\alpha M_{\mathrm{TR}} U_{\mathrm{T}} R_{\mathrm{EQ}} - 4V_{\mathrm{on}} R_{\mathrm{EQ}}}{\sqrt{\left[R_{\mathrm{R}} + R_{\mathrm{EQ}} + \alpha(\omega M_{\mathrm{TR}})^2 C_{\mathrm{F}} R_{\mathrm{F}}\right]^2 + (2\omega M_{\mathrm{RAB}})^2}} \tag{8}$$

$$P_{\mathrm{OUT}} = \frac{\left(\alpha M_{\mathrm{TR}} U_{\mathrm{T}} - \frac{8\sqrt{2}}{\pi}V_{\mathrm{on}}\right)^2 R_{\mathrm{EQ}}}{\left[R_{\mathrm{R}} + R_{\mathrm{EQ}} + \alpha(\omega M_{\mathrm{TR}})^2 C_{\mathrm{F}} R_{\mathrm{F}}\right]^2 + (2\omega M_{\mathrm{RAB}})^2} \tag{9}$$

$$\eta = \frac{P_{\mathrm{OUT}}}{P_{\mathrm{OUT}} + I_{\mathrm{F}}^2 R_{\mathrm{F}} + I_{\mathrm{T}}^2 R_{\mathrm{T}} + I_{\mathrm{R}}^2 R_{\mathrm{R}} + 4V_{\mathrm{on}} I_{\mathrm{R}}}. \tag{10}$$

It is worth noting that since the system realizes zero voltage switching (ZVS). The output voltage is proportional to M_{TR}, as shown by the equation above mentioned. Therefore, for different types of coils, interoperability, and antimisalignment performance can be achieved by simply keeping the total mutual inductance M_{TR} stable and in a reasonable range. Also, the output voltage, output power, and efficiency are inversely proportional to the cross coupling between the Rx coils. Therefore, it is necessary to eliminate the cross coupling between the Rx coils to obtain high output power and efficiency.

III. MAGNETIC DESIGN

A. Proposed Coil Structure

In order to achieve decoupling between the Rx coils, four coil structures are proposed to be used as the Rx coils, as shown in Fig. 4, and its design flow is shown in Fig. 5. The specific parameters and the turn numbers of the coils are shown in Table I. It is worth noting that the proposed coil is not limited to being an Rx coil, but can also be used as a Tx coil. There are four windings L_{AA}, L_{AB}, L_{BA}, and L_{BB}, where L_{AA} and L_{AB} form

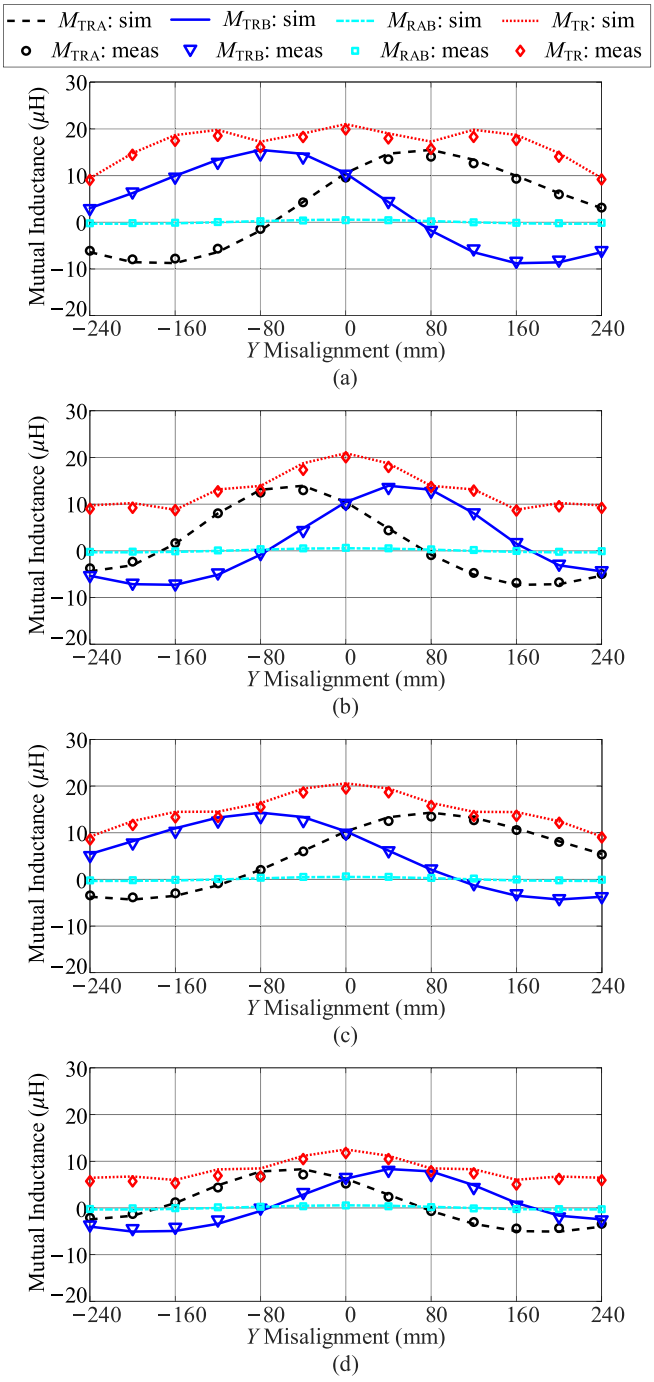

Fig. 10. Simulated and measured mutual inductances with Y misalignment with different Tx coils. (a) Square Tx coil. (b) DD Tx coil along X-direction. (c) DD Tx coil along Y-direction. (d) Quadrupolar Tx coil.

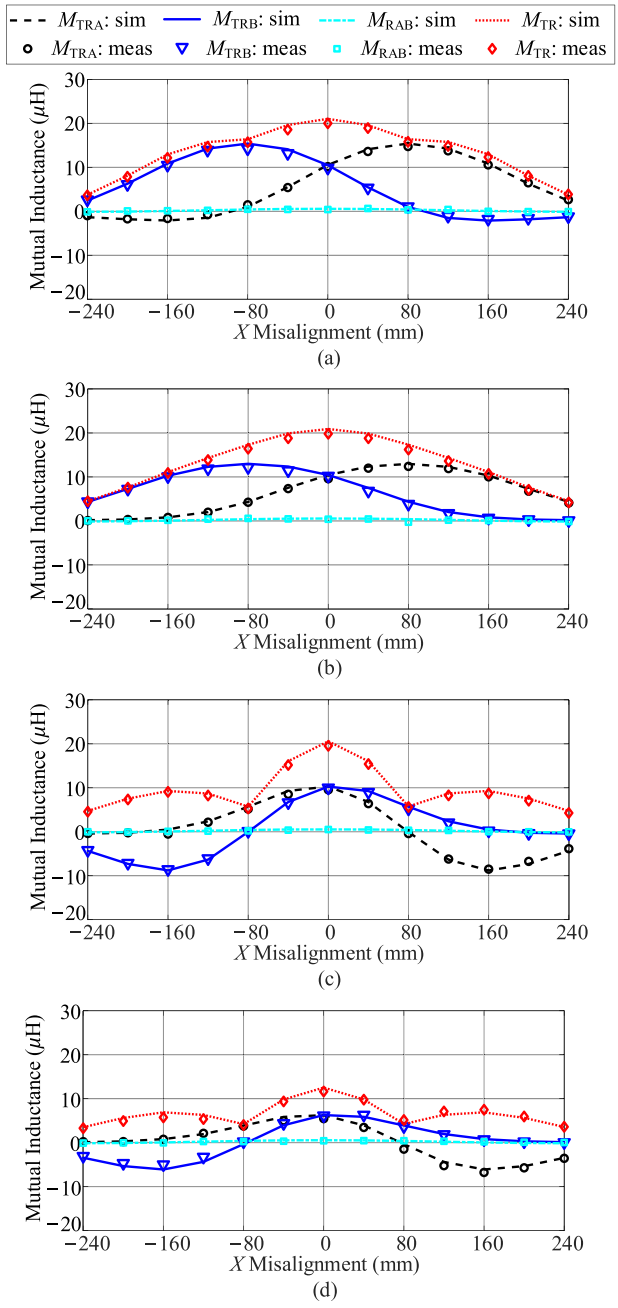

Fig. 11. Simulated and measured mutual inductances with X misalignment with different Tx coils. (a) Square Tx coil. (b) DD Tx coil along X-direction. (c) DD Tx coil along Y-direction. (d) Quadrupolar Tx coil.

Coil A, and L_{BA} and L_{BB} constitute Coil B. N_{AA}, N_{BB}, N_{AB}, and N_{BA} are the turns of the corresponding windings L_{AA}, L_{BB}, L_{AB}, and L_{BA}, respectively. Because only the location of the ferrite affects the mutual inductance between the Rx coils, and the Tx coil type is independent of this mutual inductance, the Tx coil is selected as a square coil for this paper to study the variation of the mutual inductance between the Rx coils with the misalignment. The variation of the coupling between Coil A and Coil B with misalignment for different Rx coil structures is shown in Fig. 6. As can be seen from Fig. 6, regardless of the Rx coil structure, the coupling coefficient between Coil A and Coil B fluctuates somewhat when the coil is misaligned, but the coupling coefficient is still small enough to be negligible. Therefore, it can be concluded that the proposed Rx coil structure can decouple itself.

Without losing generosity, the coil structure in Fig. 4(d), namely Structure IV, is chosen to study the decoupling. Since the proposed coil structure consists of four windings, the coupling between Coil A and Coil B can be split into the couplings among

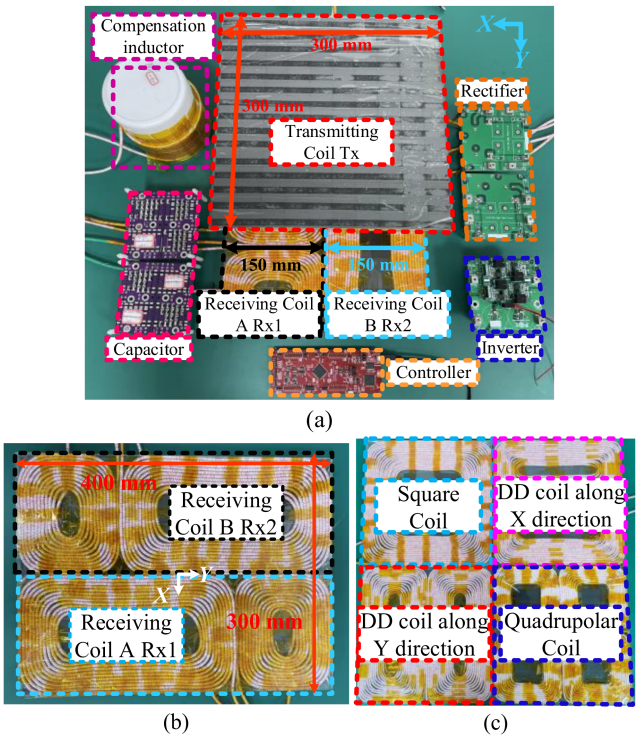

Fig. 12. Photos. (a) Experimental prototype. (b) Rx coil. (c) Tx coil.

TABLE II
PARAMETERS OF EXPERIMENTAL PROTOTYPE

V_{INV}	200 V	L_{RA}	83.04 μH	C_{RA}	42.34 nF
f	85 kHz	L_{RB}	82.95 μH	C_{RB}	42.50 nF
R_L	20 Ω	R_{RA}	0.16 Ω	R_{RB}	0.147 Ω
Square Coil		DD Coil		Quadrupolar Coil	
L_F	20.88 μH	L_F	20.88 μH	L_F	12.65 μH
L_T	156.4 μH	L_T	169.1 μH	L_T	111.1 μH
C_F	168.3 nF	C_F	168.3 nF	C_F	285.1 nF
C_T	25.89 nF	C_T	23.58 nF	C_T	35.51 nF
R_F	0.06 Ω	R_F	0.06 Ω	R_F	0.08 Ω
R_T	0.16 Ω	R_T	0.202 Ω	R_T	0.119 Ω

the four windings. The coupling between Winding L_{AA} and Winding L_{BB} is positive, and the coupling between Winding L_{AB} and Winding L_{BA} is positive, while the coupling between Winding L_{BA} and Winding L_{AA} is negative, and the coupling between Winding L_{AB} and Winding L_{BB} is negative. The decoupling between Coil A and Coil B can be achieved by reasonably adjusting the lengths, widths, and turn numbers of the windings. Take the square Tx coil as an example. The couplings among the windings are shown in Fig. 7, where k_1 and k_2 are the coupling coefficients between Windings L_{AA} and L_{BB}, L_{BA}, respectively, k_3 is the coupling coefficient between Windings L_{BB} and L_{AB}, k_4 is the coupling coefficient between Windings L_{AB} and L_{BA}, and k is the coupling coefficient between Coil A and Coil B. Because Windings L_{AA} and L_{AB} form Coil A, the coupling between them is independent of the coupling between Coil A and Coil B. The same applies to L_{BB} and L_{BA}. As can be seen

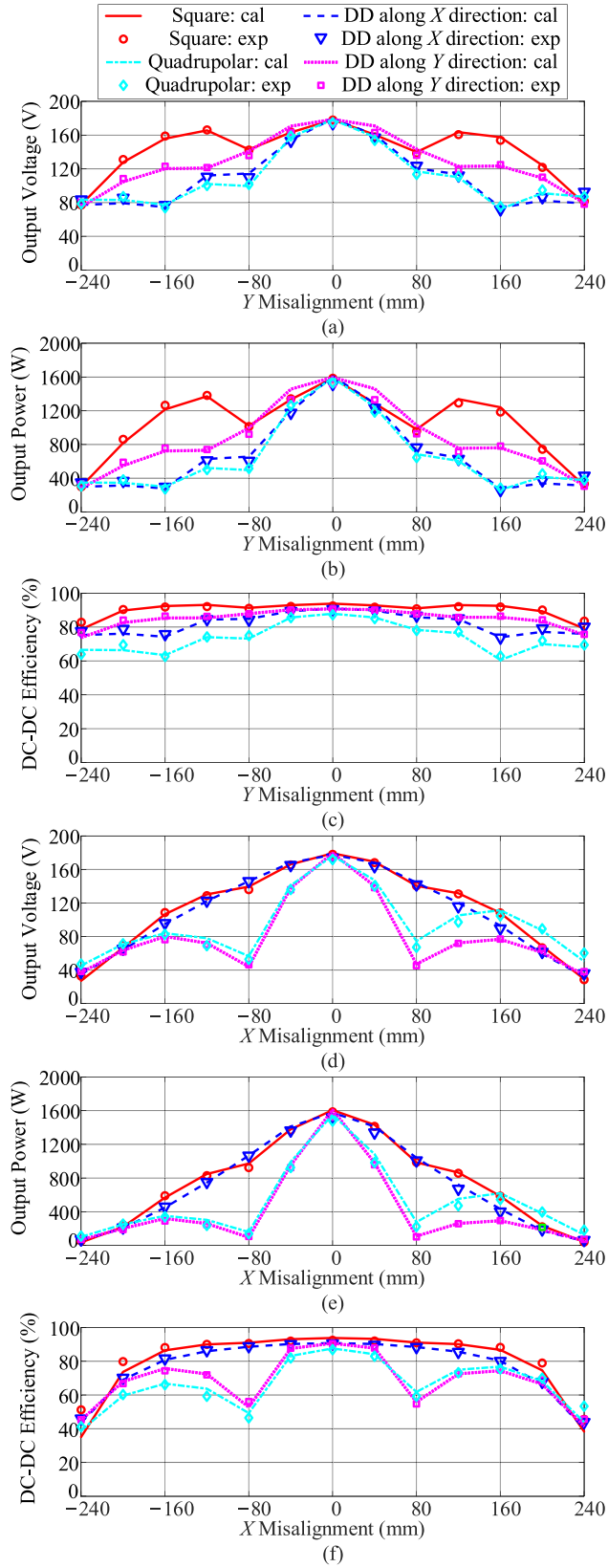

Fig. 13. Calculations and measurements with misalignment for the four different Tx coils. (a) Output voltage with Y misalignment. (b) Output power with Y misalignment. (c) DC–DC efficiency with Y misalignment. (d) Output voltage with X misalignment. (e) Output power with X misalignment. (f) DC–DC efficiency with X misalignment.

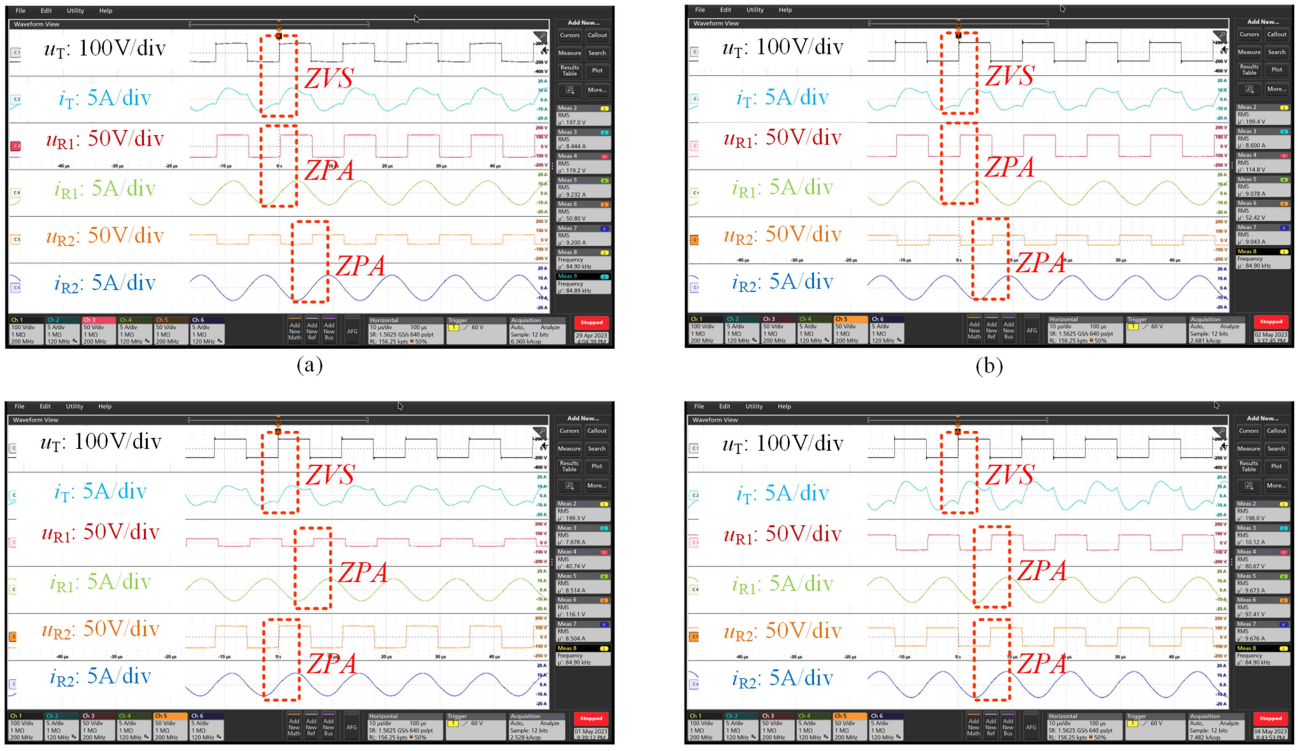

Fig. 14. Experimental waveforms. (a) Square coil as Rx coil at −120 mm *Y* misalignment. (b) DD coil along the *Y*-direction as Rx coil at 40 mm *Y* misalignment. (c) DD coil along the *X*-direction as Rx coil at −40 mm *Y* misalignment. (d) Quadrupolar coil as Rx coil at 0 mm *Y* misalignment.

in Fig. 7, decoupling between the two coils can be achieved by a reasonable design.

B. *Interoperability and Antimisalignment Analysis*

Fig. 8 illustrates the fluctuation of the mutual inductances between various Tx and Rx coils with misalignment (using the *Y*-direction misalignment as an example) when the Rx coil is a conventional coil structure, namely the square coil, the DD coil along the *X*- or *Y*-directions, and the quadrupolar coil. Fig. 8 shows that only the same type of the Tx and Rx coils have couplings when aligned. For different Tx and Rx coil types with misalignment, only one kind of the three different Tx coils have couplings with the Rx coil, while the other two kinds have zero couplings during the entire misalignment range. Meanwhile, it can be seen that the mutual inductance of the same Tx and Rx coil types decreases drastically with misalignment.

Since the two windings within one coil are wound in opposite directions, the proposed coil can have couplings with the four conventional coils in the central positions in Fig. 1, achieving interoperability. Use the different coils in Fig. 1 as the Tx coils. The variation of the total equivalent mutual inductance M_{TR} between the Tx coil and the four Rx coil structures in Fig. 4 with the *Y*-direction misalignment is shown in Fig. 9. For a fair comparison, all Rx coils mentioned herein have the same size and wire length. As can be seen in Fig. 9(a)–(d), although Structures I, II, and III can achieve partial interoperability, either the mutual inductance fluctuates too dramatic or they cannot achieve interoperability for the four conventional coils shown in Fig. 1, especially interoperability at the fully aligned positions. Therefore, Coil Structure IV is chosen as the Rx coil of the system in this paper. Meanwhile, the comparison between Figs. 8 and 9(d) shows that the proposed coil structure, compared with the conventional Rx coil structure, has smooth mutual inductance fluctuations during the misalignment range, which ensures its good misalignment tolerance. As a result, it can retain high efficiency compared with the conventional coil types. It is noteworthy that the proposed coil structure exhibits relatively weak coupling as it aims to improve interoperability and misalignment tolerance.

Figs. 10 and 11 illustrate the variation of the individual mutual inductance between various Tx and Rx coils with the misalignment when the suggested Coil Structure IV is used as the Rx coil. As can be seen from Fig. 10, although the mutual inductance between Coil A and Coil B in the proposed coil structure and the Tx coil varies with the *Y*-direction misalignment, the total equivalent mutual inductance M_{TR} between the overall Rx end and the Tx coil is limited to a reasonable range during the misalignment. In contrast, in Fig. 11, although the mutual inductance varies greatly with the *X*-direction, the system does not require much antimisalignment performance in the *X*-direction. Thus, the proposed coil structure is expected to efficiently achieve interoperability for the target four types of coils. It is worth noting that because different solenoid coils have similar magnetic fields to the unipolar or bipolar coils, the proposed coil structure is also expected to achieve

TABLE III
COMPARISONS WITH EXISTING METHODS

Ref.	Additional Control	Number of Coils	Coil Size	Anti-misalignment	Interoperability at Aligned	Interoperability			
						Square	DD along *X* Direction	DD along *Y* Direction	Quadrupolar
[11]	×	3	630×580mm	Weak	×	√	√	√	×
[12]	√	2	650×600mm	-	×	√	√	×	×
[13]	√	4	695×391mm	Strong	√	√	√	×	×
[14]	×	3	320×300mm	Strong	√	√	√	×	×
[15]	√	3	300×300mm	Weak	√	√	√	×	×
This Work	×	3	400×300mm	Strong	√	√	√	√	√

interoperability for the solenoid coils, which can be further analyzed in the future.

IV. EXPERIMENTAL VALIDATION

An experimental prototype is implemented to validate the proposal, whose photo is shown in Fig. 12. The parameters of the experimental prototype are tabulated in Table II. The overall size of the Tx coil is 300 × 300 mm, the size of the Rx coil is 300 × 400 mm, and the charging distance is 100 mm. The wire width per turn is 4.25 mm.

For four distinct Tx coils, Fig. 13 illustrates the fluctuation in the output voltage, output power, and dc–dc efficiency with misalignment. The estimated values and the experimental values are in good agreement, which supports the viability of the suggested proposal. It can be seen that the suggested Rx coil can transmit power effectively for the four typical Tx coils, namely the square coil, the DD coil along the *X*- or *Y*-direction, and the quadrupole coil, when the coils are correctly aligned. The system continues to operate at a high efficiency when a slight misalignment occurs, demonstrating the capacity of the suggested coil structure to achieve interoperability. Moreover, the output power fluctuates with the *X*-direction misalignment, but the *Y*-direction misalignment resistance is noticeably better than the *X*-direction, as can be seen from the comparison of Fig. 13(b) and (e). This is consistent with the reality that in practice, the *Y*-direction requires more adjustment and greater misalignment resistance than the *X*-direction. In Fig. 13(c) and (f), the maximum efficiency is 92.49% for the square Tx coil, 90.57% for the DD Tx coil along the *X*-direction, 90.56% for the DD Tx coil along the *Y*-direction, and 87.23% for the quadrupole Tx coil. The proposed system achieves more than 85% efficiency with the four conventional Tx coils. In addition, the system efficiency can be further increased if a better rectifier bridge and an appropriate load are chosen.

Fig. 14 shows the voltage and current waveforms for different cases in the experiments. From Fig. 14, it can be seen that the system can achieve efficient output power when the Rx coil types are different, so the system is considered to satisfy the interoperability requirement. The two output voltages will display different amplitudes with different misalignment distances. However, because of the two rectifier bridges on the Rx side being connected in series in this article, the output voltages are superimposed and the sum of their voltage amplitudes is roughly equal, so the system is deemed to meet the misalignment tolerance requirement. Meanwhile, ZVS can be achieved with the inverter.

The comparisons of this work with existing works are given in Table III. It can be concluded that the coil structure proposed in this article can achieve interoperability with the square coil, the DD coil along *X*- or *Y*-directions, and the quadrupole coil, and has good resistance to misalignment. Therefore, the WPT system proposed in this article has strong interoperability and misalignment tolerance capabilities.

V. CONCLUSION

A wireless charging system based on the mutually spliced DD coils that achieves interoperability and antimisalignment performance has been proposed in this article. These two receiving coils are connected in series via the rectifiers on the dc side, resulting in the total equivalent mutual inductance equal to the sum of the absolute values of the mutual inductances between the transmitting coil and the two receiving coils. The coils are optimized. The interoperability and antimisalignment performance of the proposed receiver with the four conventional transmitting coils, i.e., the square coils, the DD coil along *X*- or *Y*-directions, and the quadrupole coil, are evaluated and tested. The proposed solution can be a competitive solution for interoperability and misalignment tolerance.

REFERENCES

[1] A. Ahmad, M. S. Alam, and R. Chabaan, "A comprehensive review of wireless charging technologies for electric vehicles," *IEEE Trans. Transp. Electrific.*, vol. 4, no. 1, pp. 38–63, Mar. 2018.
[2] Y. Zhang et al., "Passive paralleling of multi-phase diode rectifier for wireless power transfer systems," *IEEE Trans. Circuits Syst. II, Exp. Briefs*, vol. 70, no. 2, pp. 646–649, Feb. 2023.
[3] Y. Li et al., "Extension of ZVS region of series–series WPT systems by an auxiliary variable inductor for improving efficiency," *IEEE Trans. Power Electron.*, vol. 36, no. 7, pp. 7513–7525, Jul. 2021.
[4] C. Cai, J. Wang, M. Saeedifard, P. Zhang, R. Chen, and J. Zhang, "Gyrator-gain variable WPT topology for MC-unconstrained CC output customization using simplified capacitance tuning," *IEEE Trans. Ind. Electron.*, vol. 71, no. 4, pp. 3594–3605, Apr. 2024.
[5] Y. Zhang, Z. Shen, W. Pan, H. Wang, Y. Wu, and X. Mao, "Constant current and constant voltage charging of wireless power transfer system based on three-coil structure," *IEEE Trans. Ind. Electron.*, vol. 70, no. 1, pp. 1066–1070, Jan. 2023.

[6] Y. Zhang et al., "A quadrupole receiving coil with series-connected diode rectifiers for interoperability of nonpolarized and polarized transmitting coils," *IEEE Trans. Power Electron.*, vol. 38, no. 7, pp. 8000–8004, Jul. 2023.
[7] Y. Zhang, C. Liu, M. Zhou, and X. Mao, "A novel asymmetrical quadrupolar coil for interoperability of unipolar, bipolar, and quadrupolar coils in electric vehicle wireless charging systems," *IEEE Trans. Ind. Electron.*, vol. 71, no. 4, pp. 4300–4303, Apr. 2024.
[8] R. Xie, R. Liu, X. Chen, X. Mao, X. Li, and Y. Zhang, "An interoperable wireless power transmitter for unipolar and bipolar receiving coils based on three-switch dual-output inverter," *IEEE Trans. Power Electron.*, vol. 39, no. 2, pp. 1985–1989, Feb. 2024.
[9] Y. Chen et al., "A clamp circuit-based inductive power transfer system with reconfigurable rectifier tolerating extensive coupling variations," *IEEE Trans. Power Electron.*, vol. 39, no. 2, pp. 1942–1946, Feb. 2024.
[10] W. S. Lee, W. I. Son, K. S. Oh, and J. W. Yu, "Contactless energy transfer systems using antiparallel resonant loops," *IEEE Trans. Ind. Electron.*, vol. 60, no. 1, pp. 350–359, Jan. 2013.
[11] A. Bilal, G. Covic, and S. Kim, "Interoperability of magnetic pads with intermediate coils and different primaries," in *Proc. Wireless Power Week*, 2022, pp. 497–502.
[12] G. Yang et al., "Interoperability improvement for rectangular pad and dd pad of wireless electric vehicle charging system based on adaptive position adjustment," *IEEE Trans. Ind. Appl.*, vol. 57, no. 3, pp. 2613–2624, May/Jun. 2021.
[13] B. E. Jamakani, E. Afjei, and A. Mosallanejad, "A novel triple quadrature pad for inductive power transfer systems for electric vehicle charging," in *Proc. 10th Int. Power Electron., Drive Syst. Technol. Conf.*, 2019, pp. 618–623.
[14] W. Li, J. Lu, G. Zhu, W. Zhang, and J. Jiang, "Design and research of a double-sided flux coupler in inductive power transfer system," in *Proc. IEEE 42nd Annu. Conf. Ind. Electron. Soc.*, 2016, pp. 6033–6037.
[15] Y. Zhang, W. Pan, H. Wang, Z. Shen, Y. Wu, and X. Mao, "Interoperability study of wireless charging system with unipolar and bipolar coils based on capacitor–inductor–capacitor–Capacitor–Series topology," *Energy Rep.*, no. 8, pp. 405–411, Aug, 2022.
[16] R. Bukya, B. Mangu, B. Bhaskar, and B. Bhavsingh, "Analysis of interoperability different compensation network in wireless EV charging systems," in *Proc. 2nd Glob. Conf. Advance. Technol.*, 2021, pp. 1–6.
[17] D. Kraus, M. Hassler, G. Covic, and H.-G. Herzog, "Impedance based design method for interoperable wireless power transfer systems," in *Proc. IEEE Energy Convers. Congr. Expo.*, 2021, pp. 1580–1587.
[18] D. Kraus, G. A. Covic, H.-G. Herzog, P. A. J. Lawton, and F. J. Lin, "Design and assessment of an interoperable wireless power transfer system using an impedance-based method," *IEEE Trans. Power Electron.*, vol. 38, no. 2, pp. 2768–2781, Feb. 2023.
[19] G. Yang et al., "Improved interoperability evaluation method for wireless charging systems based on interface impedance," *IEEE Trans. Power Electron.*, vol. 36, no. 8, pp. 8588–8592, Aug. 2021.
[20] J. Xu, S. Wang, Y. Zhang, C. Xu, and B. Wei, "Interoperability testing coil for EV wireless power transfer system," in *Proc. IEEE 4th Int. Future Energy Electron. Conf.*, 2019, pp. 1–6.
[21] Standardization Administration of China, "Electric vehicle wireless power transfer-Part 6: Interoperability requirements and testing-Ground side," Standardization Administration of China, Tech. Rep. GB/T 38775.6, 2021.
[22] Standardization Administration of China, "Electric vehicle wireless power transfer-Part 7: Interoperability requirements and testing-Vehicle side," Standardization Administration of China, Tech. Rep. GB/T 38775.7, 2021.
[23] "Wireless power transfer for light-duty plug-in/electric vehicles and alignment methodology," Int. Standard SAE J2954, 2020. [Online]. Available: https://www.sae.org/standards/content/j2954_202010/
[24] Y. Zhang, W. Pan, H. Wang, Z. Shen, Y. Wu, and X. Mao, "Misalignment-tolerant dual-transmitter electric vehicle wireless charging system with reconfigurable topologies," *IEEE Trans. Power Electron.*, vol. 37, no. 8, pp. 8816–8819, Aug. 2022.
[25] K. Song et al., "Design of DD coil with high misalignment tolerance and low EMF emissions for wireless electric vehicle charging systems," *IEEE Trans. Power Electron.*, vol. 35, no. 9, pp. 9034–9045, Sep. 2020.
[26] E. S. Lee, B. H. Choi, Y. H. Sohn, G. C. Lim, and C. T. Rim, "Multiple dipole receiving coils for 2-D omnidirectional wireless mobile charging under wireless power zone," in *Proc. IEEE Energy Convers. Congr. Expo.*, 2015, pp. 3209–3214.
[27] Y. Zhang, S. Chen, X. Li, and Y. Tang, "Design methodology of Free-Positioning nonoverlapping wireless charging for consumer electronics based on antiparallel windings," *IEEE Trans. Ind. Electron.*, vol. 69, no. 1, pp. 825–834, Jan. 2022.
[28] Y. Wu, C. Liu, M. Zhou, X. Mao, and Y. Zhang, "An antioffset electric vehicle wireless charging system based on dual coupled antiparallel coils," *IEEE Trans. Power Electron.*, vol. 38, no. 5, pp. 5634–5637, Mar. 2023.
[29] Y. Chen et al., "A hybrid inductive power transfer system with misalignment tolerance using Quadruple-D quadrature pads," *IEEE Trans. Power Electron.*, vol. 35, no. 6, pp. 6039–6049, Jun. 2020.
[30] G. Ke, Q. Chen, S. Zhang, X. Xu, and L. Xu, "A single-ended hybrid resonant converter with high misalignment tolerance," *IEEE Trans. Power Electron.*, vol. 37, no. 10, pp. 12841–12852, Oct. 2022.
[31] W. Shi et al., "Design of a highly efficient 20-kW inductive power transfer system with improved misalignment performance," *IEEE Trans. Transp. Electrific.*, vol. 8, no. 2, pp. 2384–2399, Jun. 2022.

Wenbin Pan was born in Quanzhou, China. He received the bachelor's degree in electrical engineering and automation from Hebei Normal University, Shijiazhuang, China, in 2020. He is currently working toward the master's degree in electrical engineering with Fuzhou University, Fuzhou, China.

His research interests include high frequency converters and wireless power transfer.

Chao Liu was born in Shanxi, China, in 1997. He is currently working toward the Ph.D. degree in power electronics with the School of Electrical Engineering and Automation, Fuzhou University, Fuzhou, China.

His research interests include power electronics converters and wireless power transfer.

Hongmin Tang was born in Fujian, China. He is currently working toward the master's degree in power electronics with the School of Electrical Engineering and Automation, Fuzhou University, Fuzhou, China.

His research interest includes wireless power transfer.

Yizhan Zhuang (Member, IEEE) was born in Fujian, China, in 1994. He received the B.S. degree in electrical engineering from the College of Electrical Engineering and Automation, Fuzhou University, Fuzhou, China, in 2017 and the Ph.D. degree in electrical engineering from the School of Electrical Engineering, Wuhan University, Wuhan, China, in 2023.

He is currently a Lecturer (Associate Researcher) with the School of Electrical Engineering and Automation, Fuzhou University, Fuzhou, China. His research interests include dc–dc power converter and interface of photovoltaic conversion systems.

Yiming Zhang (Senior Member, IEEE) received the B.S. and Ph.D. degrees in electrical engineering from Tsinghua University, Beijing, China, in 2011 and 2016, respectively.

Afterwards, he was a Postdoctoral Researcher with San Diego State University, San Diego, CA, USA and a research fellow with Nanyang Technological University, Singapore. He is currently a Full Professor with Fuzhou University. He has authored 1 book from Springer, authored or coauthored more than 100 technical papers in journals and conference proceedings. His research interests include wireless power transfer and resonant converters.

Dr. Zhang was the recipient of the Outstanding Doctoral Dissertations of Tsinghua University in 2016. He was recognized as an Outstanding Reviewer for the IEEE TRANSACTIONS ON POWER ELECTRONICS in 2019 and 2022, and a Distinguished Reviewer for IEEE TRANSACTIONS ON INDUSTRIAL ELECTRONICS in 2020. He was the Publication Chair of the international conference ICWPT2022.